Georg-August-Universität
Göttingen

Project 6: Model for the Spread of Infectious Diseases

Carlo von Carnap

Summer Term 2023

Final Project *Scientific Computing*,
Salvatore R. Manmana

Supervisor: Emily Klass

Submission Date: 08.08.2023

Contents

1 Introduction

Infectious disease modelling describes the process of applying mathematical models to predict the future state of an epidemic. It has surged in popularity during the COVID-19 pandemic and its influence on recent policies has been overwhelming, despite its mediocre success in projecting reality. The difficulties when modelling infectious diseases range from the overcomplex real situations to finding suitable assumptions to keep an appropriate level of accuracy. Generally it can be distinguished between macroscale models such as the SEIR-model[1] that apply differential equations on a population level, and microscale models that have individuals as their smallest unit.

This model uses a cellular automaton[2] of quadratic shape $L \times L$ as well as stochastic methods to examine the spread of an infectious agent on a microscale. Each grid node is occupied by an immobile person and can be in one of the states Susceptible S, Infected I, or Recovered R. Later, the fourth state Vaccinated V is introduced. It is a stationary state that permanently excludes people from taking any of the three other states. For a person in one of the three active states S, I, and R, three transitions are follow with their respective probabilities p_1, p_2, and p_3:

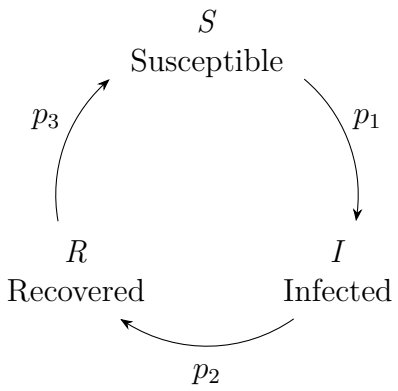

- p_1: a susceptible person getting infected by an infected neighbor
- p_2: an infected person turning recovered
- p_3: a recovered person returning susceptible

For the $S \to I$ transition, a von Neumann neighborhood was applied, meaning the four immediately adjacing nodes are consideres as neighbors.[2] Vaccinated people V are set at the beginning of the simulation, with p_4 being the probability that a spot is occupied by one. The other three states are initialized with the same likelihood, as the simulation steps progress by each updating L^2 randomly chosen nodes according to the above mentioned rules.

Goal was now to use this model to examine the influence of the transition probabilities on the infection rates averaged over all simulation steps. This included varying the $S \to I$ turover rate p_1 for different combinations of $p_2\,(I \to R\,)$, and $p_3\,(R \to S)$ as well as using different vaccination rates p_4 at initialization. For all simulations, different grid sizes were used to observe potential statistical inaccuracies.
Further, the time evolution of the infection rates was looked at to stress the validity of the preceding time averaging. Therefore a quantity of 20 infection rate samples was

generated over simulation time with mean and standard deviation calculated for each timestep.

2 Theory

2.1 Averaging within Simulation Runs

Fundamental to the analysis of the simulation results is the rate of infected individuals in the grid at each timestep $\langle I \rangle_t$. It is calculated by summing up the infection status $I_{i,j}$ over the totality of the grid and dividing it by the number of grid nodes L^2,

$$\langle I \rangle_t = \frac{1}{L^2} \sum_{i=1,\, j=1}^{L} I_{i,j}. \tag{2.1}$$

For that, the infection status is either taking $I_{i,j} = 1$ for the person being in state I or $I_{i,j} = 0$ otherwise. This infection rate can now be averaged over all timesteps t to receive

$$\overline{\langle I \rangle} = \frac{1}{T} \sum_{t=0}^{T} \langle I \rangle_t, \tag{2.2}$$

the time-averaged infection rate which most of the analysis steps are based on.

2.2 Averaging across Simulation Runs

For the evaluation of the time-averaging, the infection rate $\langle I \rangle_t$ was also averaged over a multitude of N samples for each timestep. This mean at a given timestep t is calculated as

$$\overline{\langle I \rangle_t} = \frac{1}{N} \sum_{n=1}^{N} \langle I \rangle_t \tag{2.3}$$

and posesses a standard deviation of

$$\sigma_{\langle I \rangle_t} = \sqrt{\frac{1}{N} \sum_{n=1}^{N} \left(\langle I \rangle_t - \overline{\langle I \rangle_t} \right)^2}. \tag{2.4}$$

3 Methodology

3.1 Pseudorandom Number Generator (PRNG) MT19937

For the generation of pseudorandom numbers, the 1997 developed PRNG Mersenne Twister MT19937[3] was chosen. It was published in 1997 and has become one of the most popular PRNGs across programming languages.[4]

Its very long period with $2^{19937} - 1$ integers as well as the fact that its random numbers are highly equidistributed[5], make the Mersenne Twister a very strong choice. The Mersenne Twister broadly works by first taking a vector of 624 random numbers as seed, then transforming it applying a "twist" operation and subsequently using it to retrieve the usable pseudorandom number. Once all integers of the state vector are consumed, the vector is regenerated.[4][6]

4 Implementation

4.1 Integration of External Libraries

Alongside the C standard library headers, the `gsl_rng.h` of the GNU Scientific Library (GSL) as well as the two numeric libraries `cvc_numerics.h` and `cvc_rng.h` were included in the project. Of the standard library, the header files `stdio.h`, `stdlib.h`, `tgmath.h` and `time.h` were used, the GSL header `gsl_rng.h` was only accessed to generate pseudorandom nubers.

The `cvc_numerics.h` of the two own libraries provides mainly numerical methods for differentation, integration or to solve differential equations, while the `cvc_rng.h` offers functions requiring PRNGs. This includes for instance Monte-Carlo integrators or tools helpful to analyse stochastic datasets such as calculating mean or standard deviation of given arrays.

4.2 Structure and Workflow of the Main Program

4.2.1 Generation of Random Numbers by a Static PRNG

For the generation of pseudorandom numbers, the in Subsection 3.1 described Mersenne Twister MT19937 of the GSL library was used. It was implemented statically to generate uniformly distributed numbers in the interval $[0, 1)$ and can therefore be accessed globally by the respective functions.

Overall the PRNG was used in two different ways, once to obtain probabilities, other to generate random integers. The former was accomplished by checking if the uniform was smaller than the respective probability, the latter by multiplying the uniform by the largest desired integer and then casting it to `int`.

4.2.2 Implementation of the Modelling Grid

The above mentioned grid itself was realized as a $(L+2) \times (L+2)$ heap section of integer values, with L being the sidelength of the quadratic grid where the actual spread of the infection takes place. While this section is technically one-dimensional, it will for simplicity reasons be here referred to as a two-dimensional structure of the given shape. Inside the grid, the following integer values were used to model the different states of the people within the simulation:

- `0`: this person is Susceptible S to the infection
- `1`: the person is Infected I
- `2`: the person is Recovered R and currently not susceptible
- `-1`: the person is Vaccinated V and does not participate in the spread

The grid was implemented with a supporting edge of ghosts at the top, bottom, left and right border, that are neither infectious nor subject to any updates of the grid — they will permanently take the value `0` and are irrelevant for the later visualization and analysis of the data.

4.2.3 Functions Acting on the Modelling Grid

In the main program all changes in the grid are facilitated by functions outside the main one. They entirely work with or change the grid in-place and all take the grid itself as well as its length $L + 2$ as arguments. Inside the functions, the grid is refered to as `grid` and its length as `length`, while the above probabilities are passed in form of the double array `probabilities` having p_1, p_2, p_3, and p_4 as its entries. Excluding the ones to calculate the infection rate and its time average, none of the functions does have a return value. Overall the following functions can be called from the main:

- `void print_grid`: prints the passed grid as terminal ouput
- `void grid_init`: initializes the grid applying the vaccination probability
- `void update_node`: updates the given node selected by its $L \times L$ grid coordinates `row_i` and `column_j` according to the turnover probabilities
- `void grid_update_linear`: calls the `update_node` function for each node in order of their grid position
- `void grid_update_stochastic`: calls `update_node` for L^2 randomly chosen nodes
- `double ratio_infected`: calculates the ratio of infected individuals with respect to the total grid population for a given grid
- `double average_ratio_infected`: applies `T` simulation steps to the grid by calling the stochastic grid updater with passed turnover probabilities and averages the calculated infection rate over each simulation step

4.2.4 Structure of the Main Function and Generated Data Files

The main function is divided into compartements for each individual analysis step, where every compartment is a local scope in order to prevent the variables from interfering with each other. Therefore each one uses its own variables, files and grids, with the latter being then shaped by calling the functions from Subsection 4.2.3. The files are also being written at directly from the main function.

The first compartment itself uses the command line interface to take the probabilities p_1, p_2, p_3, and p_4 as well as the grid size L as user input. Further it can be specified how the grid is going to be updated. Either all grid nodes are updated sequentially (for user input `0`) or L^2 grid nodes are selected randomly. After initializing the grid, individual actualization steps can be performed manually according to the previously selected simulation scheme by pressing `ENTER` until the loop is quit with `q` confirmed by `ENTER`. While here the mechanism to update the grid is subject to the users input, for the following simulation tasks the model operates using the stochastic updating method for each timestep (i.e. L^2 random nodes are selected for actualization). It was chosen to avoid adding a spatial bias by having a pre-selected order; however, in terms of results, there is no meaningful difference expected between the two schemes.

The remainder of the program runs independently from the user, **overall a running time of around three minutes should be expected after the interactive part is finished**. The majority of the time is comsumed by the second scope, generating

the data files for the p_1 dependency of time-averaged infection rate $\overline{\langle I \rangle}$ without vaccinations. The files do each have the respective grid size in column one and the values of p_1 written in the first row. The data points are the time-averaged infection rates for the previous parameters and calculated using the corresponding calculation function for $T = 1000$. Overall three files are being written at in the `/soi_data` directory, one for each combination of p_2 and p_3:

- `soi_average_ratio_infected_over_p1_a.csv`: $p_2 = 0.3$, $p_3 = 0.3$
- `soi_average_ratio_infected_over_p1_b.csv`: $p_2 = 0.6$, $p_3 = 0.3$
- `soi_average_ratio_infected_over_p1_c.csv`: $p_2 = 0.3$, $p_3 = 0.6$

The data file generated by the third compartment for $p_1 = p_2 = p_3 = 0.5$,

- `soi_average_ratio_infected_over_p4_v.csv`,

uses a similar structure. Here the vaccination rate occupies the first row, with the columns once again using the same grid sizes as before.

For the time development of the infection rate, an additional heap section is used to support the statistical analysis across data samples. It has the data series for each time as virtual rows, that are then passed to the respective `cvc_rng.h` functions to calculate mean and standard deviation. The data file of the this third scope,

- `soi_ratio_over_time.csv`,

has the sample number as fist column and the timestep as first row, the data points are the infection rates of each sample and timestep. Mean and standard deviation have extra rows at the end of the file marked with `00` and `01` respectively instead of the sample number.

Addinitionally, three data files resembling the state of the grid itself are generated into the `/soi_animations` folder:

- `soi_grid_over_time_a.csv`
- `soi_grid_over_time_b.csv`
- `soi_grid_over_time_c.csv`

Therefore the dimensionality of the used two-dimensional 96×96 grid is reduced to one and for each timestep occupying the first column of the files, the grid state is a one-dimensional data series behind it. For the representation of the state of each individual node, the same notation as described in Subsection 4.2.3 is used.

5 Results and Discussion

5.1 Ratio of Infected People Averaged over Time

Aim was now to analyse the infection rate inside the grid averaged over all timesteps $\overline{\langle I \rangle}$ for different combinations of p_1, p_2 and p_3. To achieve this, the dependency of the turnover probability $p_1\,(S \to I)$ on the time-averaged infection rates was simulated for different combinations of $p_2\,(I \to R)$ and $p_3\,(R \to S)$. The simulation was performed over $T = 1000$ simulation steps for each of the grid sizes $L = 16$, $L = 32$, $L = 64$ and $L = 128$.

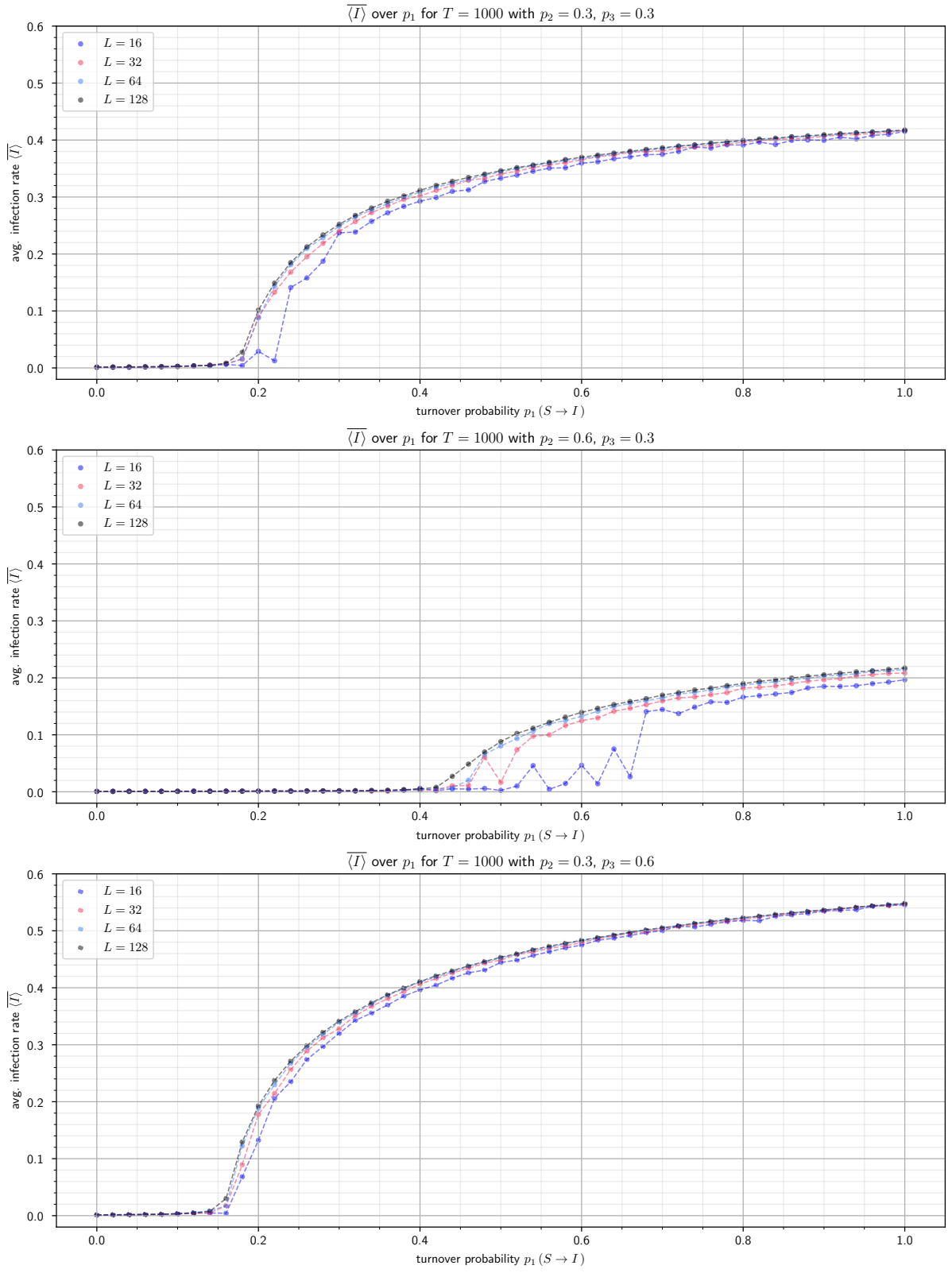

Figure 1: Plots showing the time-averaged infection rates $\overline{\langle I \rangle}$ in dependence of the turnover probability $p_1\,(S \to I)$ for the different grid sizes $L = 16$, $L = 32$, $L = 64$ and $L = 128$ with $T = 1000$ simulation steps each. The upper plot was generated using the turnover rates $p_2\,(I \to R) = 0.3$ and $p_3\,(R \to S) = 0.3$, the middle one using $p_2 = 0.6$ and $p_3 = 0.3$, and the lower one $p_2 = 0.3$ and $p_3 = 0.6$.

The latter grid size $L = 128$ is the largest one used for any simulation and still takes an acceptable but still non-negligable amount of calculation time. Since this side length should provide more than fluctuation-resistant results and the calculation time more than doubles for a doubling in L due to the calculation functions, this was the maximum grid size trialed.

From looking at the results shown in Figure 1 it immediately becomes visible that the lower grid sizes undergo stronger fluctuations in $\overline{\langle I \rangle}$ than the higher ones, with very strong deviations for $L = 16$, particularly with $p_2 = 0.6$ and $p_3 = 0.3$. It is worth noting that the lower grid sizes only deviate towards smaller time-averaged infection rates and never towards higher ones. This can be explained by the underlying reason behind the deviations, which is not in fact primarily attributed to statistical fluctuations — those are kept to a minimum due to averaging over time — but rather a secondary effect of the stochastic methods: the spread came to a halt after the number of infected individuals had fluctuated to zero at some point during the simulation. The occurance of these zeroed runs does obviously happen more frequently with smaller grids, which can be confirmed using the manual updater at the beginning of the program and operating it with even lower grid sizes such as $L = 8$. Since the final time-averaged infection rate also correlates with the timestep where the spread eventually stopped (and earlier halts are more likely with lower infection rates), stronger outliers also follow as more frequent for low infection rates. Consequently the simulation ran with $p_2 = 0.6$ and $p_3 = 0.3$ and therefore the lowest $\overline{\langle I \rangle}$, also underwent the biggest changes from $L = 16$ in comparison with higher grid sizes.

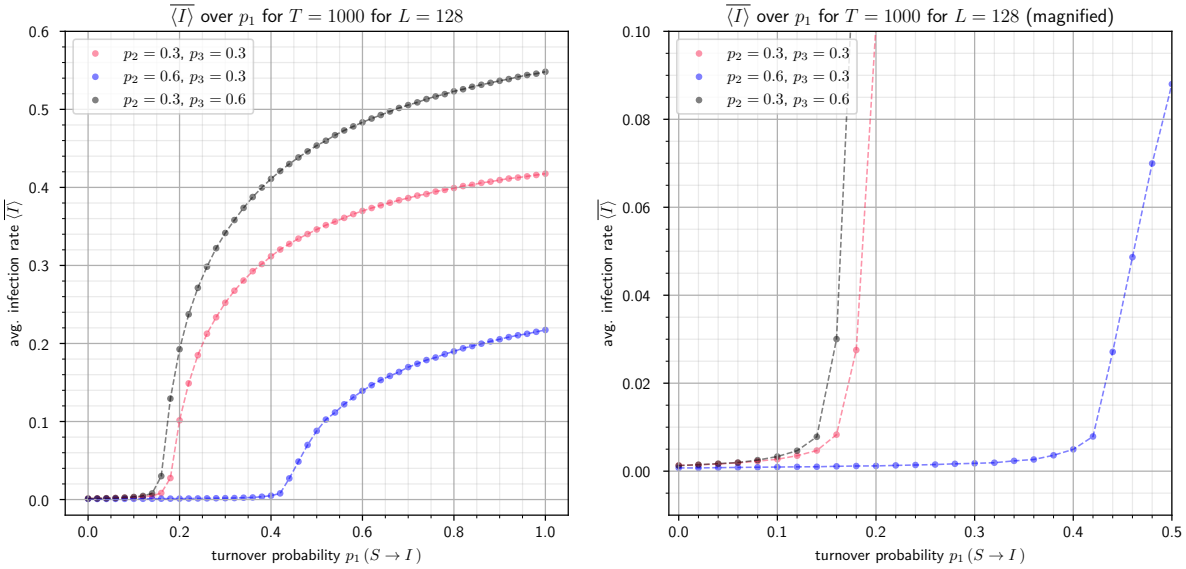

Figure 2: Detailed view of the time-averaged infection rates $\overline{\langle I \rangle}$ over $p_1\,(S \to I)$ for $L = 128$ and $T = 1000$ simulation steps. On the left the different trends for the respective choices of $p_2\,(I \to R)$ and $p_3\,(R \to S)$ can be observed, while on the right the critical values of p_1 for $\overline{\langle I \rangle}$ approaching zero are emphasized.

To further focus on the variations for different values of p_2 and p_3, as well as the exact shape of the plotted curves, the time-averaged infection rates $\overline{\langle I \rangle}$ for the different probability combinations are shown together in Figure 2. The plots only comprise the grid size $L = 128$ for better visibility, while the biggest grid size was chosen for accuracy reasons.

Qualitatively it can be seen that $\overline{\langle I \rangle}$ remains approximately zero until a critical probability $p_1\,(S \to I)$ is reached and then experiences a rise leading to a maximum value at $p_1 = 1$. The critical value of the the time-averaged infection rate becoming non-zero, as well as the maximum value of $\overline{\langle I \rangle}$ differ between the different combinations of $p_2\,(I \to R)$ and $p_3\,(R \to S)$. Specifically, that means we receive larger maximum values of $\overline{\langle I \rangle}$ for $I \to R$ transitions being more likely and smaller maximum $\overline{\langle I \rangle}$ values for likelier $S \to I$ turnover rates. This corresponds to the intuitive understanding of the problem: there are more infected individuals when infections occur more frequently (hence the rise in $\overline{\langle I \rangle}$ for increased p_1) or when people are sooner capable of getting (re) infected and overall less infected individuals for recoveries becoming more likely. For the critical probability p_1 it can be observed that it is significantly higher for the likelier $I \to R$ transition ($p_1 \approx 0.4$) but remains approximately the same ($p_1 \approx 0.14$) for the two values of $p_3\,(R \to S)$. To explain this, an extreme case with very low infection rates around the critical p_1 value must be imagined. In such a case it will obviously matter how long people are infectious as it directly increases the likelihood of a neighbor getting infected. However, with the infection rate itself being very low, the rate of recovered individuals will also be very low and their recovery probability therefore will only have a very limited influence on the amount of infections happening. That being said, the influence — albeit very low — does exist, which is why in Figure 2 also a slight difference in the critical p_1 value regarding the halting of the spread can be observed between the different probabilities of p_3.
Comparing this to the results regarding the maximum value of $\overline{\langle I \rangle}$, it can be said that the $p_3\,(R \to S)$ rate gains importance for higher infectction rates, while recovery rate p_2 and infection rate p_1 affect the spread regardless of the state the model is in.

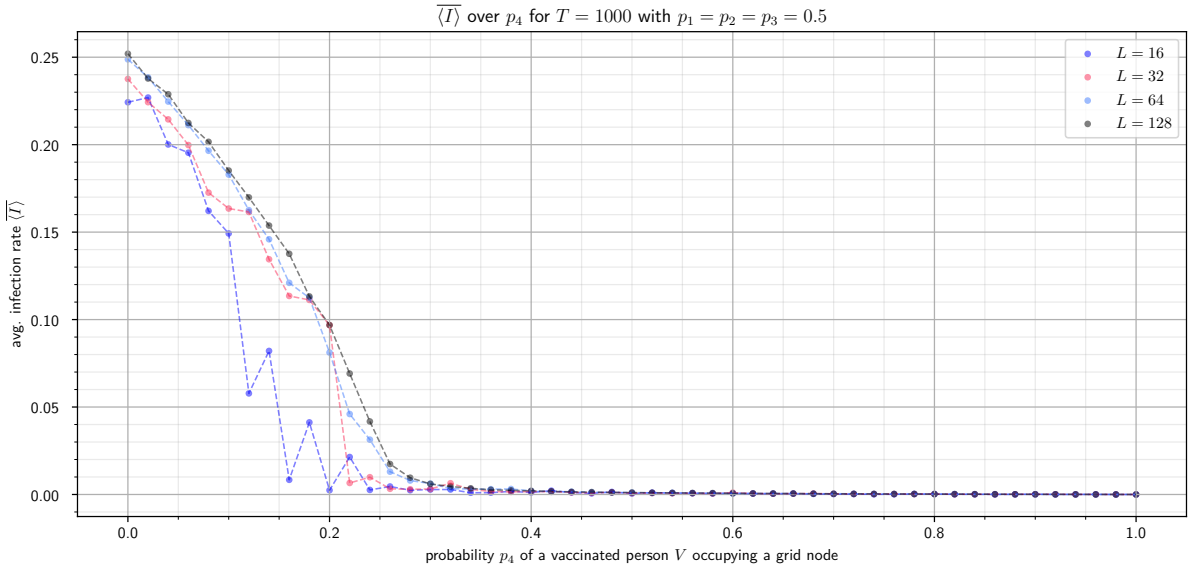

Figure 3: Display of the time-averaged infection rates $\overline{\langle I \rangle}$ depending on the vaccination rate p_4 at the beginning of the simulation and constant turnover probabilities $p_1 = p_2 = p_3 = 0.5$. The simulation was performed over $T = 1000$ simulation steps and th respective grid sizes $L = 16$, $L = 32$, $L = 64$ and $L = 128$.

5.2 Influence of Vaccinated People on the Spread

In this simulation part, permanently vaccinated individuals V were introduced. To investigate their influence of the infectious spread, the vaccination rate p_4 was varied between values of zero and one and its influence on the infection rate — again averaged over simulation time — was calculated for $p_1 = p_2 = p_3 = 0.5$. Like previously, a total of $T = 1000$ simulation steps for the grid sizes $L = 16$, $L = 32$, $L = 64$ and $L = 128$ were conducted and can be observed in Figure 3.

It can be seen that the time-averaged infection rate has an original value of around $\overline{\langle I \rangle} = 0.25$ for $p_4 = 0$ and then decreases until a vaccination rate of approximately $p_4 = 0.3$ is reached. At that vaccination rate the spread vanishes entirely. Again, the different grid sizes are subject the previously descibed deviations. The results match the expectations, the more individuals are excluded from the spread via vaccination, the less people are infected. Worth noting is the exact vaccination rate that halts the spread, which is rather low.

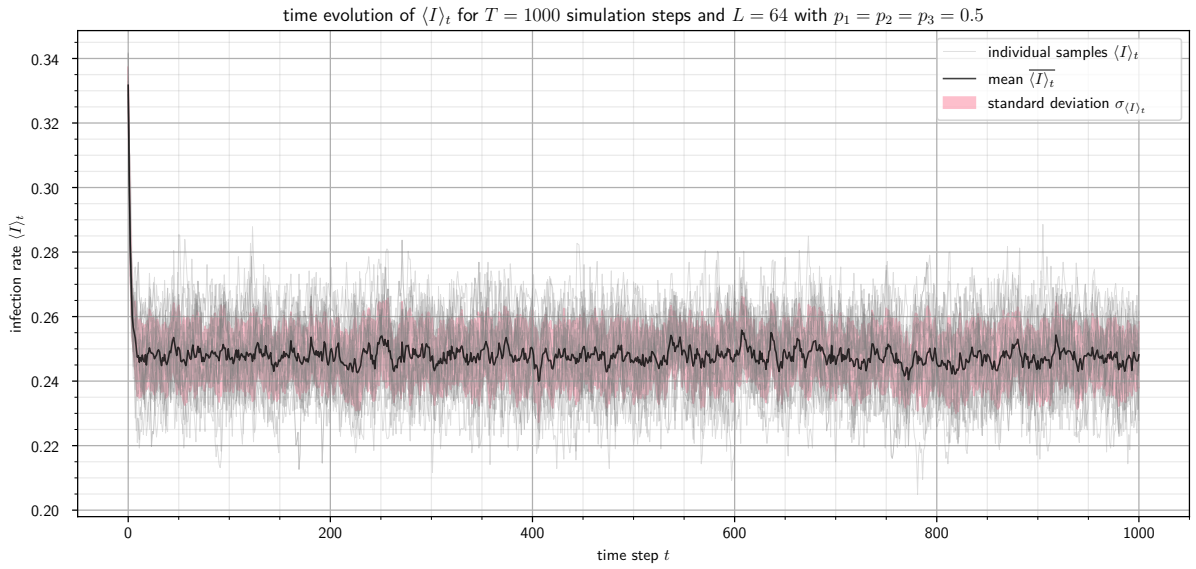

Figure 4: Time evolution of the infection rate $\langle I \rangle_t$ over each of the $T = 1000$ simulation steps for a total of 20 samples. At each timestep mean $\overline{\langle I \rangle_t}$ and standard deviation $\sigma_{\langle I \rangle_t}$ of the infection rate were calculated and are also highlighted in the plot. The grid size was chosen as $L = 64$, the turnover probabilities as $p_1 = p_2 = p_3 = 0.5$, no vaccinated induviduals were used.

5.3 Time Evolution of the Infection Rate

In the preceding subsections the average of the ratio of infected individuals has been taken over time. For this calculation to yield meaningful results, it is necessary to have rather time-stable infection rates over the course of the simulation. For that matter, the focus should now be layed on the time development of the infection rate $\langle I \rangle_t$ itself. Overall $N = 20$ samples were generated, while a grid size $L = 64$ was chosen for an appropriate balance between running time and accuracy. The number of simulation steps again was set to $T = 1000$, as turnover probabilities $p_1 = p_2 = p_3 = 0.5$ were chosen without vaccinated individuals at initialization. Further, the mean of the infection rates $\overline{\langle I \rangle_t}$ and

as its standard deviation $\sigma_{\langle I \rangle_t}$ were calculated for each simulation step. This allows for a more detailed analysis of the statistical fluctuations in the infection rates $\langle I \rangle_t$ across samples.

The results are displayed in Figure 4 and it becomes immediately visible that a stable state, only subject to statistical fluctuations, is reached after only a few simulation steps. Consequently, the initial state of the grid differing in infection rate from the stable state, will only have a limited influence on the eventual time average. This underlines the validity of the time averaging used in the pervious analysis steps.

6 Supplementary Materials

Several animations of the spread progressing over time were rendered using the python library manim[7] and can be found in the directory `/soi_animations`. As seen in the exemplary video frame in Figure 5, the aminations use a 96×96 grid size. The probabilities were varied to offer a broader understanding of different situations.

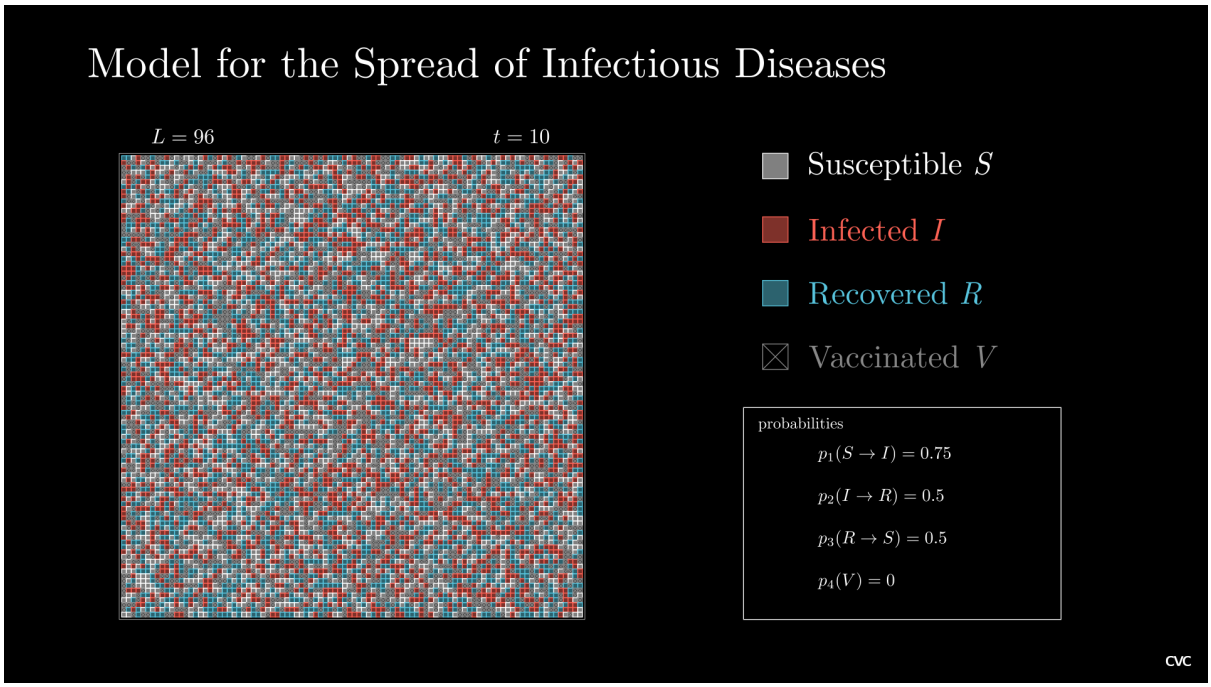

Figure 5: Frame $t = 10$ of an animated simulation of the infectious disease model for the grid size $L = 96$. The grid was initialized with a vaccination rate $p_4 = 0.25$ and progressed with the turnover probabilities $p_1 = 0.75$ as well as $p_2 = p_3 = 0.5$. The total animation as well as variations in the probabilities can be found under `/soi_animations`.

Literature

[1] Cornelis P. Dullemond. *EpiDemo. SEIR-Type models.* URL: https://www.ita.uni-heidelberg.de/~dullemond/software/epidemo/seirmodels.html (visited on 07/31/2023).

[2] Debasis Das. "A Survey on Cellular Automata and Its Applications". In: vol. 269. Dec. 2011. ISBN: 978-3-642-29218-7. DOI: 10.1007/978-3-642-29219-4_84.

[3] Makoto Matsumoto and Takuji Nishimura. "Mersenne Twister: A 623-Dimensionally Equidistributed Uniform Pseudo-Random Number Generator". In: *ACM Trans. Model. Comput. Simul.* 8.1 (1998). ISSN: 1049-3301. DOI: 10.1145/272991.272995. URL: https://doi.org/10.1145/272991.272995.

[4] *educative. What is Mersenne Twister?* URL: https://www.educative.io/answers/what-is-mersenne-twister (visited on 07/29/2023).

[5] Alex. *Learn C++. Generating random numbers using Mersenne Twister.* July 28, 2023. URL: https://www.learncpp.com/cpp-tutorial/generating-random-numbers-using-mersenne-twister/ (visited on 08/02/2023).

[6] David Wong. *www.cryptologie.net. How does the Mersenne's Twister work?* Feb. 2016. URL: https://www.cryptologie.net/article/331/how-does-the-mersennes-twister-work/ (visited on 08/02/2023).

[7] *The Python Package Index. manim.* URL: https://pypi.org/project/manim/ (visited on 08/03/2023).